Labels, Thresholds and the Reference Itself: Evaluating Sentinel-1 Flood Segmentation Against Copernicus EMS Maps, with a Preregistered Blind Test

Teo Clerici Jurado
BSc in AI & Data Science, H-FARM College / University of Chichester
Correspondence: clerici.teo5@gmail.com
An independent research project, not part of the degree's coursework.

Code and reports: https://github.com/teo-clerk/floodfusion
Frozen weights: https://huggingface.co/teo-clerk/floodfusion
Interactive Arena and live maps: https://teo-clerk.github.io/floodfusion/

This is a non-peer-reviewed preprint submitted to EarthArXiv.
November 2026. Release v1.3.0 (doi:10.5281/zenodo.24194785); blind-test models frozen at tag v1.2.0-freeze. Extends the v1.2 preprint of 15 October 2026.

Abstract. Flood-segmentation models for Sentinel-1 synthetic aperture radar (SAR) are usually ranked by cross-validation on benchmark chips whose labels share sensors, dates and definitions with the model inputs. We measure how far such scores carry to operational reference maps, what limits them there, and whether adapting a model to the reference helps. The reference is Copernicus Emergency Management Service (CEMS) rapid mapping: the delineations of 38 flood activations from 2023 to 2026 drawn on non-Sentinel radar satellites, against which every model is applied, without training on these events, at its own calibrated threshold. A gated cross-attention SAR–optical fusion model that scores 0.608 IoU in leave-one-event-out cross-validation on Sen1Floods11 scores 0.266 on these maps, below a physics baseline (0.373); trained on Kuro Siwo's flood labels, the same architecture scores 0.407. Our v1.2 model adds a seasonal Sentinel-1 reference and is trained on 7,006 chips from 138 floods (Kuro Siwo and GEOID-Flood). It scores 0.417 IoU, against 0.405 for TerraMind-base adapted with LoRA to the same labels and tuning budget, and 0.419 against 0.321 for Copernicus's Global Flood Monitoring (GFM) ensemble on the 34 activations GFM covers, with GFM's exclusion mask scored as dry. At each activation's best threshold in hindsight, our model would reach 0.468. The reference is itself uncertain: consecutive CEMS delineations of the same area, made 6–24 h apart, agree with each other at 0.520 macro IoU over 34 activations; on the 27 activations in both sets, the model scores 0.433 and the consecutive products 0.536. Adapting to the reference does not close the remaining gap. In grouped cross-validation over the 38 activations, a threshold refitted on the other folds gains 0.002, and fine-tuning on their CEMS labels loses 0.041 (0.380 against 0.421), so an adoption rule fixed in advance adopted neither. Because this benchmark had been seen during development, all of these comparisons are exploratory. The confirmatory test is preregistered: every eligible CEMS flood activation from EMSR899 on is scored by models frozen at a git tag, and the hashes of the sealed scores are committed to a hash-chained ledger until 20 activations in 15 clusters are scored, or until the end of 2027. The frozen weights are public and drive a service that maps new floods from Sentinel-1, showing the model's map with no reference and no score. We also report two errata in our earlier results.

Keywords: flood mapping; Sentinel-1; synthetic aperture radar; Copernicus Emergency Management Service; reference data; geospatial foundation models; TerraMind; preregistration; blind test

1 Introduction

Radar is central to flood mapping: the weather that floods a valley is the weather that clouds it, and the C-band synthetic aperture radar (SAR) on Sentinel-1 sees the ground through cloud, day and night. Two Copernicus services map floods operationally. Rapid mapping by the Emergency Management Service (CEMS) produces on-demand delineations for each activation, drawn by analysts on satellite imagery ranging from very-high-resolution commercial images to Sentinel data [1]. The Global Flood Monitoring (GFM) product runs an ensemble of three algorithms on every Sentinel-1 acquisition, worldwide and automatically [2, 3]. Deep-learning segmentation models trained on benchmark data sets—Sen1Floods11 [4], Kuro Siwo [5] and, recently, GEOID-Flood [6]—and geospatial foundation models such as TerraMind [7] are proposed as more accurate alternatives.

Such claims are mostly measured by cross-validation on benchmark chips. Spatial dependence between training and test data is known to inflate such estimates [8–10], and flood benchmarks add couplings of their own: Sen1Floods11's labels were drawn mostly on the Sentinel-2 image that a fusion model also receives, and they mark water on a date rather than flood. Recent comparisons also suggest that the encoder matters less than its reputation. PANGAEA finds that foundation models do not consistently outperform supervised baselines [11]; GEOID-Flood reports a consistent but modest advantage for them [6]; and in a global evaluation of fine-tuned TerraMind, a U-Net reached higher recall than every TerraMind configuration, at slightly lower accuracy and precision [12].

We ask five questions. **(Q1)** How far do cross-validation scores carry to independent operational maps? **(Q2)** Does a task-specific model with radar context beat a fairly adapted foundation model, and the operational GFM product? **(Q3)** How well does the reference agree with itself? **(Q4)** Does adapting a model to the reference's own labels close the gap? **(Q5)** How can such claims be tested without the test set shaping the model? We address Q1, and Q2 descriptively, on a

benchmark of 38 CEMS flood activations from 2023–2026, fixed by a preregistered rule before any model was scored on it (release v1.2). Q3 and Q4 are answered on the same seen benchmark under a second protocol, committed before any of its numbers existed (release v1.3). Because that benchmark was seen during development, our answers there are exploratory. A preregistered blind test, now running, will answer Q2 confirmatorily; it is also our answer to Q5. Our contributions are:

- A measured gap between cross-validation and independent operational maps. Sen1Floods11-trained optical models fall from about 0.6 IoU in leave-one-event-out cross-validation to 0.27–0.30, below a physics baseline. The training data, labels included, move scores far more than the architecture or the optical input (Section 5.1).
- A seasonal-context model (v1.2) and a fair foundation-model opponent: TerraMind-base with LoRA, a siamese pre/post input, its DEM and an equal tuning budget, trained on the same pool of 138 floods. On the CEMS maps the two nearly tie (0.417 vs 0.405). An apparent 0.08 IoU advantage in cross-validation was mostly threshold transfer (Sections 5.2–5.3).
- An exploratory comparison with Copernicus GFM on the floods it covers (0.419 vs 0.321). The gap lies more in GFM's fixed decision rule, exclusion mask included, than in how its likelihood ranks pixels (Section 5.4).
- A measurement, which we have not found published, of how well consecutive CEMS delineations of the same flood agree: 0.520 macro IoU over 34 activations, against the models' 0.42. Per activation, the model's score is associated with that agreement (post hoc, Spearman $\rho = 0.51$; Section 5.5).
- An adaptation ladder with an adoption rule fixed in advance. Neither a threshold refitted on other CEMS floods (+0.002) nor fine-tuning on their labels (−0.041) was adopted (Section 5.6).
- A preregistered blind test on CEMS activations that no model had seen, with hash-committed scores and a power analysis (Section 6), and the frozen model released with a service that maps new floods from each Sentinel-1 pass, under rules that keep the blind test intact (Section 7).
- Two errata in our own earlier results (Section 4.5), and an account of the project's provenance and of how an AI coding agent was used to build and audit it (Section 9).

2 Related work

SAR flood mapping. Operational SAR flood mapping thresholds the low backscatter of calm water, compares the image with a reference acquisition, and masks terrain where flooding is implausible, for instance by the height above the nearest drainage (HAND) [13]. GFM combines three such algorithms into an ensemble flood extent with a per-pixel likelihood [2, 3], and ships an exclusion mask where SAR cannot see flooding: radar shadow, layover, dense vegetation and built-up areas.

Benchmarks. Sen1Floods11 pairs Sentinel-1 chips with hand-labelled water from 11 events [4]. Kuro Siwo provides flood polygons drawn on Sentinel-1 for multi-temporal flood mapping [5]. GEOID-Flood, derived from CEMS activations, spans 219 events in 65 countries, with pre- and post-event Sentinel-1, a pre-event Sentinel-2 composite, a DEM and validated labels that separate permanent water from flood [6].

Foundation models. TerraMind is an any-to-any generative multimodal model pre-trained on nine geospatial modalities [7]; TerraTorch packages it, with other geospatial foundation models, for fine-tuning [14]. Low-rank adaptation (LoRA) [15] lets a large encoder adapt on a small GPU. Where no seasonally matched pre-event image is available, context helps across backbones: on two held-out US flood events, AlphaEarth embeddings [16] and a DEM each improved single-date SAR segmentation for four backbones, TerraMind among them [17].

Reference data. SAR flood maps are validated against analyst delineations or against water mapped on a near-simultaneous optical image, and the reference is usually taken as truth. CEMS rapid-mapping products are generalised maps, drawn under time pressure on whatever images are available [1]. Agreement between annotators is a standard check of segmentation labels in other fields, but to our knowledge no published study measures how well two CEMS delineations of the same flood agree.

Evaluation practice. We borrow two practices from fields whose evaluation sets are scarce and reused: spatially grouped validation [8, 10], and preregistration, in which hypotheses, analyses and stopping rules are committed before the outcomes that will test them have been observed [18].

3 Data

3.1 Inputs

Every input is fetched from Microsoft Planetary Computer [19], with no account or key. The inputs are:

- Sentinel-1 radiometrically terrain-corrected backscatter γ^0 (VV, VH) of the post-event pass, and of the latest same-orbit pass up to 60 days earlier;
- Sentinel-2 L2A bands B3, B8 and B11, with a per-pixel quality from the scene classification;
- the Copernicus GLO-30 DEM, from which slope, HAND, the local incidence angle, radar shadow and layover are derived;
- JRC Global Surface Water [20] for permanent water, and ESA WorldCover [21] for analysis.

All layers are resampled to one 10 m UTM grid on the SAR geometry. Training chips are 256×256 pixels (2.56 km).

3.2 Training sets

Sen1Floods11 (v1.0, v1.1) supplies hand labels of water. We use them as flood, after removing JRC permanent water, on 10 of its 11 events; Paraguay's acquisition is missing from the archive. **Kuro Siwo** (v1.1, v1.2) supplies flood polygons drawn on radar, for 36 events in 29 groups of events within 100 km. v1.1 also built Sen1Floods11-like water labels on

the same chips (Section 5.1). **GEOID-Flood** (v1.2, revision `868407460bf3`) supplies 111 events from before EMSR656 that Kuro Siwo lacks, of which 102 produced chips (`reports/v1_2_deviations.md`). Its class 2 is flood and its class 1 permanent water. A square must have at least 50 % labelled pixels.

The **v1.2 pool** joins the two flood-label sets. It holds 7,006 chips from 827 stacks of 138 floods, in 81 location groups formed by 100 km single linkage across both sets. The largest group holds 13.6 % of the windows, below the 25 % threshold, fixed before any run, for switching to buffered spatial blocks. Cross-validation is grouped five-fold, and each group is tested once by a model that never saw it.

3.3 The CEMS 2023–26 benchmark

v1.1's preregistered protocol fixed the benchmark before any v1.1 model was trained. A census of codes EMSR656–EMSR898 found 233 public activation records, 86 of them floods. One rule applied to every delineation product:

- all of its source images are non-Sentinel: radar such as COSMO-SkyMed, PAZ, RADARSAT-2, TerraSAR-X or ICEYE, or very-high-resolution optical such as Pléiades or WorldView;
- its package is published;
- a Sentinel-1 acquisition lies within ±24 h of its latest image and covers at least half of its extent;
- a same-orbit pre-event acquisition exists.

44 activations with 117 areas of interest (AOIs) qualified. Each activation keeps at most four AOIs, and each AOI at most 16 tiles, drawn by a seeded generator blind to the flood and to every model. That leaves 90 (product, pass) pairs on 605 tiles. A pixel is scored if it lies inside the product's observed region, has valid SAR and is outside permanent water.

The *primary stratum* holds the products drawn on radar satellites: the conservative test for an optical input. Excluding EMSR664 (Forlì, a case study before v1.1) leaves 38 activations, with 75 pairs and 3,395 km^2 (original tiles) of mapped flood. Of these pairs, 34 were drawn on very-high-resolution images (CEMS class VHR2) and 41 on coarser images (class HR+). One storm can trigger several activations, so activations within 100 km and 60 days of each other (single linkage) form clusters: 30 of them. Every result is reported at both unit definitions.

3.4 Copernicus GFM as a comparator

We read GFM from the EODC STAC catalogue, anonymously. For each pair we take the GFM item of the exact post-event Sentinel-1 frame, matched by acquisition start time, and resample its ensemble flood extent (binary) and ensemble likelihood (0–100) onto the tile grid by nearest neighbour. GFM is never a model input.

- **Coverage.** 557 of the 605 tiles have a GFM product. Eight pairs have none: six are Sentinel-1C frames from before GFM began processing Sentinel-1C in October 2025, and two are Sentinel-1A frames.
- **Versions.** The tiles span GFM v3.1.0 (328), v4.0.0 (24) and v4.1.0 (205).
- **Units.** A unit counts for GFM only where GFM covers at least 95 % of its scored pixels, so that missing GFM pixels do not count as misses. 69 of the 75 primary pairs qualify, giving 34 activations in 26 clusters.

3.5 v1.3: the benchmark's labels, and consecutive delineations

Copernicus's own labels for training. v1.3's ladder (Section 4.4) trains on the benchmark's labels, which follow the blind test's definition of flood exactly. It uses every pair of the benchmark except EMSR664's: 89 pairs from 43 activations, 30,834 chips of the rebuilt stacks. Testing and selection use the primary stratum only (75 pairs, 38 activations, 27,501 chips). Training and validation also use the 14 pairs whose products were drawn wholly or partly on optical images, a choice the author made before any run, for more training data. A pixel trains and scores only where the scorer would score it, and its label is the product's observed flood, so training and scoring share one pixel definition.

Groups. Activations whose footprints lie within 100 km of each other form one group, whatever their dates (single linkage), so a place mapped twice never both trains a model and tests it. There are 34 groups, 30 of them with radar-drawn pairs; the largest holds 12.4 % of the chips, below the 25 % rule. Four of the 30 clusters of Section 3.3 span two folds: their activations' tiles lie more than 100 km apart, so a fold model can train on one activation of a storm and be tested on another activation of the same storm, in a different place. This was disclosed before any ladder number existed.

Consecutive delineations. For the reference ceiling we take, in every AOI of the seen flood activations (EMSR656–898), each pair of consecutive delivered delineation products whose latest source images are at most 24 h apart: the benchmark's own window between a product and its Sentinel-1 pass. A metadata probe had counted 111 pairs in 45 activations, but 221 of the 883 dated delineation products have no download path (an AOI product never made), and only delivered products are maps. That leaves 80 pairs in 34 activations, fixed before any product was compared. One package returns HTTP 404, so 79 pairs are compared. No code from EMSR899 on is read.

4 Methods

4.1 Models

The physics baseline uses no learning. Every learned model shares one training recipe and one decision rule (Section 4.2).

Physics baseline (row 2). A tile-adaptive backscatter threshold is combined with a change term against the pre-event pass and with terrain masks (HAND, slope, radar shadow and layover, permanent water). One offset is set on Sen1Floods11 validation data.

SAR U-Net (row 4). A U-Net [22] on Sentinel-1 backscatter alone. It reads no terrain and no optical input.

Gated cross-attention fusion (row 9). Two encoders (64–512 channels, GroupNorm) read, respectively, the SAR stack with terrain (slope, log(1+HAND), local incidence) and the

Table 1: Data sets, their roles and their use. "Seen" means that the data informed development: only the blind set can test the hypotheses.

Data set	Role	Labels or content	Size used	Licence
Sen1Floods11 [4]	training (v1.0, v1.1)	hand-labelled water, drawn mostly on Sentinel-2	10 events	none declared; not redistributed
Kuro Siwo [5]	training (v1.1, v1.2)	flood polygons drawn on Sentinel-1	36 events, 29 groups	CC BY (data), MIT (code)
GEOID-Flood [6]	training (v1.2)	flood and permanent water, validated	102 events before EMSR656	CC BY 4.0
v1.2 pool	training, CV	flood minus permanent water	7,006 chips, 138 floods, 81 groups	—
CEMS 2023–26	evaluation (seen)	analyst delineations on non-Sentinel imagery	38 activations, 30 clusters, 75 pairs	© EU, CEMS terms
Copernicus GFM	comparator	ensemble flood extent and likelihood	34 activations, 26 clusters	© EU, CEMS terms
CEMS, all strata	ladder (v1.3)	as CEMS, drawn on radar or optical	89 pairs, 43 activations, 34 groups	© EU, CEMS terms
CEMS product pairs	ceiling (v1.3)	two delineations of one AOI, ≤ 24 h apart	79 pairs, 34 activations	© EU, CEMS terms
Blind set (EMSR $\geq$ 899)	confirmatory test	as CEMS	accruing	© EU, CEMS terms

optical bands (B3, B8, B11, MNDWI). The SAR stack has five channels: VV and VH after and before the event, and their VV difference. At 1/8 resolution the optical features query the SAR features through eight attention heads. A learned per-pixel gate $g = \sigma\big(\mathrm{MLP}([q; F_o; F_s])\big) \in [0, 1]$, a function of the optical quality q and both feature maps, adds the result to the SAR stream:

$$F = F_s + g \odot \mathrm{Attn}\big(Q = F_o,\, K = F_s,\, V = F_s\big). \qquad (1)$$

With the gate closed, the output is exactly that of the network's own SAR-and-terrain path. Missing optical is a learned embedding, never zeros, and per-sample modality dropout ($p = 0.5$) trains the SAR-only path. A U-Net decoder (256 to 32 channels) produces the flood logits.

v1.2: seasonal context (row 21). The seasonal reference lets the model ask not only *is this pixel water?* but *is this water unusual for this place and season?* A sidecar layer holds it: the median, in linear power, of every same-orbit Sentinel-1 acquisition within ±30 days of the same date one year earlier, taken over at least three scenes. It contributes three channels, VV and VH of the seasonal reference and VV after the event minus VV seasonal (in dB), normalised with fixed data-set statistics. They enter the SAR-and-terrain encoder with an availability channel. Where a stack has no reference, the model substitutes a learned constant per channel, and context dropout ($p = 0.3$) trains that case. The reference exists for 731 of the 827 pool stacks (88 %) and for 595 of the 605 CEMS tiles (98 %). The motivation came from v1.1's diagnostics. On Sen1Floods11 the recent pre-event pass, 5–24 days before the image, was often already flooded. Replacing it with the seasonal reference lifted the physics baseline by +0.175 IoU on Sen1Floods11 and by +0.087 on Kuro Siwo. It did not help on CEMS (0.340 vs 0.371, v1.1 tiles), whose recent reference had been chosen to precede the activation. An AlphaEarth context (rows 20 and 22) was planned and deferred, before any context model was trained: reading the embeddings from the public mirror took minutes per band and failed under parallel requests.

Fair TerraMind (row 24). v1.1's TerraMind saw a single date through a frozen encoder. The v1.2 opponent is TerraMind-1.0-base [7], used through TerraTorch [14]: the largest variant in a size rule fixed beforehand for an 8 GB GPU. TerraMind-large was not tried.

- **Siamese input.** One encoder runs twice with shared weights. The post-event pass reads Sentinel-1 VV and VH, Sentinel-2 B3, B8 and B11 where usable (clouded pixels set to the pre-training mean) and the GLO-30 DEM, TerraMind's native terrain modality. The pre-event pass reads Sentinel-1 alone.
- **Adaptation.** LoRA [15] of rank 8 ($\alpha = 16$) adapts the attention projections. The LoRA update starts at zero, so at initialisation the encoder is the pre-trained one.
- **Head.** The tokens of blocks 3, 6, 9 and 12 of both passes are concatenated, reshaped into a pyramid and decoded by a U-Net decoder (256 to 32 channels).
- **Shared rules.** Modality dropout is row 9's, and the neck and decoder run once per batch (the erratum 1 fix, Section 4.5).

Size and adaptation followed a rule logged before any result. Base with LoRA was to be used unless a timing probe projected more than 3 h per pooled cross-validation run, with base frozen and then small with LoRA as the fallbacks. The probe projected 0.40 h at 2.9 GB of peak reserved memory, so base with LoRA was used. It trains 20.4 M parameters, against 18.2 M for row 9. Figure 1 shows both architectures.

4.2 Training, calibration and selection

Recipe. Every learned model minimises a focal plus Dice loss with AdamW and a warm-up and cosine schedule. It trains for at most 30 epochs, stopping early (patience 8) on the validation macro IoU, with an effective batch of 16 in bfloat16.

Equal tuning budget. Each family tried the same three learning rates (3×10^{-5}, 10^{-4}, 3×10^{-4}) on an inner split of fold 0's training groups. Row 9 chose 3×10^{-4}, which row 21 inherits without tuning of its own. TerraMind chose 10^{-4}.

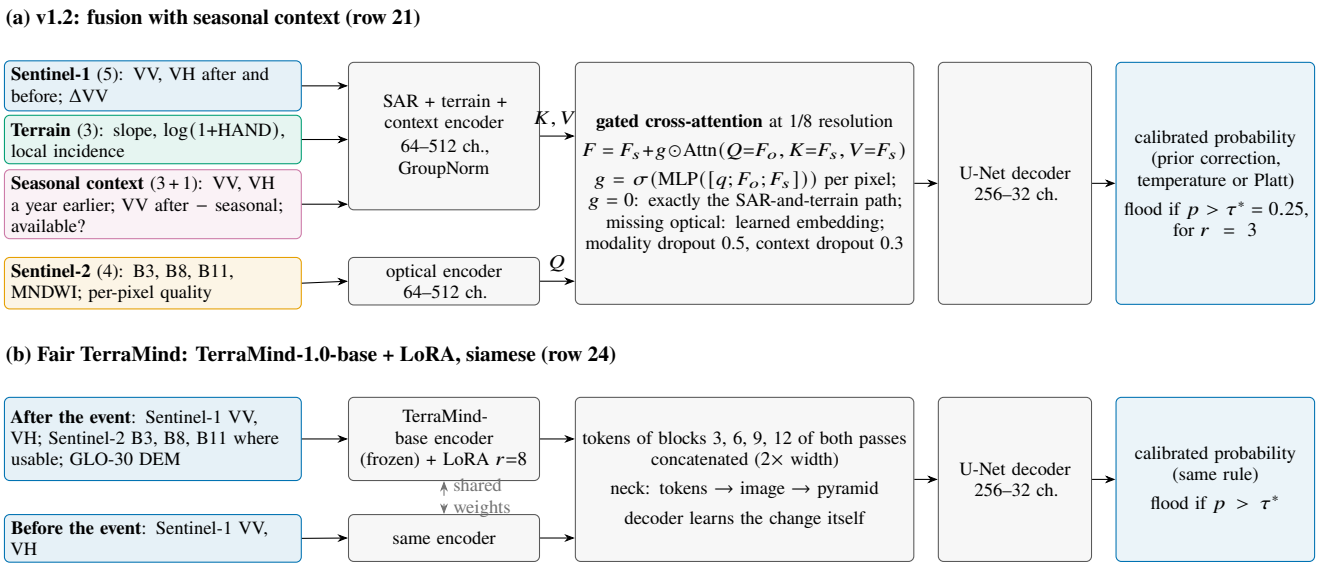


Figure 1: The two systems compared in v1.2. Both are trained on the same pool of 138 floods, with the same loss, schedule, sampler, calibration and threshold rule. (a) Our model reads terrain and a seasonal Sentinel-1 reference beside the flood image. (b) The fair TerraMind reads its native modalities, including a pre-event image and its DEM. The comparison is of system against system: what each reads is part of the comparison.

Calibration and threshold. Calibration is fitted on validation data only: an analytic correction of the prior shift that the sampler introduces, then temperature scaling [23], replaced by Platt scaling [24] when that lowers the validation log-loss by more than a set margin. A pixel is flooded when its calibrated probability exceeds $\tau^* = 1/(1+r)$, with a stated miss-to-false-alarm cost ratio $r = 3$, so $\tau^* = 0.25$. Because each model's calibration is its own, so is the threshold on its raw score. The pipeline also produces a conformal recall threshold [25], which is not evaluated here.

Selection. The candidates were row 9 and row 21, compared in pooled cross-validation on whole test stacks (the deployment operator) as macro IoU at τ^* over the 79 groups with flooded pixels; row 21 had to beat row 9 by more than 0.005. It won, 0.380 to 0.361, better in 49 of the 79 groups. Two inference add-ons had to raise that mean by at least 0.005 and help a majority of groups:

- per-scene self-calibration, a bounded EM prior shift [26], changed it by −0.042;
- a HAND cut at 15 m changed it by +0.001 and helped 30 of the 79 groups.

Neither was adopted.

Final models. Each final model trains on four of the five folds (63 groups, 5,605 chips). The fifth fold's other 17 groups (617 chips) set early stopping, calibration and the deployment prior. Each model has three seeds (42, 43, 44).

4.3 Metrics and statistics

IoU per unit. A unit is an activation or a cluster. Its IoU comes from the confusion counts pooled over its AOIs, tiles and seeds at each model's own τ^*, and the macro average over units is reported. We also report three companions:

- the *oracle* IoU, at each unit's best threshold in hindsight;
- the *self-calibrated* IoU, after a per-scene EM prior shift bounded at $|\Delta\text{logit}| \le 2$;
- the threshold-free average precision (AP).

These three are computed per seed from per-unit histograms of the calibrated probability, then averaged over seeds. The histograms have 256 bins equally spaced in logit over $[-10, 10]$, so a threshold resolves to 0.078 logit.

Tests. A gap between two models is the mean per-unit difference. We test it with a two-sided sign-flip test, exact up to 20 units and by Monte Carlo with 200,000 patterns above; every CEMS test here has at least 26 units. p-values are Holm-adjusted [27] within each unit definition, and a result counts only if it holds at both. Intervals are 95 % bootstrap intervals over units.

4.4 v1.3: the reference ceiling and the adaptation ladder

v1.3's protocol was committed on 10 November 2026, before any v1.3 model was trained and before any ceiling or ladder number was computed. It was written with v1.2's results on this benchmark known, and they motivated the ladder, so every v1.3 number on it is exploratory.

The reference ceiling. Both products of a pair are rasterised on a 10 m grid in the AOI's UTM zone, over the intersection of their observed regions, and their observed-flood layers are compared. A pair's IoU is that of the two maps; an activation's IoU pools its pairs' pixel counts; the ceiling is the macro mean over activations. It is broken down by the time between the two products' latest images (< 6 h, 6–24 h), by sensor pair and by whether the two share a source image. A sensitivity row drops the pairs whose later product repeats more than 5 % of its flood area from images no later than the earlier product's; two maps that share polygons agree by construction. The reading was fixed in the protocol: agreement near 0.5 means the benchmark is near its ceiling, near 0.8 that most of the gap is the models'. Floods also change within 24 h, so the ceiling includes real change, as the benchmark's ±24 h tolerance between a product and its pass does. It is descriptive and has no p-value.

The adaptation ladder. Three rungs are scored on the same 38 activations, each activation by the fold that held out its group (grouped five-fold; fold i tests, fold i+1 validates, the other three train). Every rung uses row 21's seed 42:

- **R1, zero-shot:** row 21 at its own τ^*.
- **R2, recalibration:** R1's scores, with the threshold refitted as the argmin of 3 FN+FP (the cost ratio that defines τ^*) on the pooled pixel counts of every radar-drawn pair outside fold i.
- **R3, fine-tuning:** row 21's weights trained further on fold i's three training folds (about 18,500 chips), with row 21's loss, sampler, augmentation, schedule (at most 30 epochs, patience 8) and normalisation. Calibration, prior and τ^* are fitted on the validation fold, as for every model here. The learning rate was chosen from 10^{-5}, 3×10^{-5} and 10^{-4} by v1.2's tuning rule on an inner split of fold 0: 10^{-5}, by a margin of 0.00001 in validation macro IoU over 10^{-4}.

The measure is macro IoU over the 38 activations from binned counts; as a code check, R1 with all three seeds reproduces row 21's committed binned score, 0.418 (Section 5.3). **The adoption rule:** R2 is adopted over R1 if it gains at least 0.005 *and* is better on more than half of the 38 activations; R3 is adopted over the highest rung adopted below it by the same rule. The highest adopted rung would have become v1.3's model, frozen and entered in the blind test as H8 (Section 6). If no rung is adopted, there is no v1.3 model, the null result is reported and H8 is not run. Clusters, AP and the oracle threshold are reported descriptively. An optional pass of the fair TerraMind through the same ladder was not run.

4.5 Two errata

Both defects came to light during v1.2's planning and data preparation, after v1.1 had been reported. Each is documented with its evidence, a regression test and a re-measurement.

Erratum 1: TerraMind trained without modality dropout. TerraMind's configuration set modality dropout to 0.5, as for the fusion model, but the training loop applied dropout only to the fusion architectures. TerraMind therefore trained with $p = 0$, so its SAR-only path, which most CEMS pixels need, was barely trained. Its BatchNorm layers also saw sub-batches of one to three chips. v1.1 had reported fusion beating TerraMind on CEMS (H4) by +0.031 per activation (Holm $p = 0.034$) and +0.039 per cluster ($p = 0.009$). In a post-hoc re-run on the same, already seen benchmark (unadjusted p), TerraMind-small retrained as described rises from 0.226 to 0.299 IoU, and the comparison reverses: fusion minus TerraMind is −0.042 [−0.065, −0.018] per activation (fusion better on 10 of 38, $p = 0.001$) and −0.043 per cluster ($p = 0.003$). The preregistered verdict stands as run, and its conclusion is withdrawn.

Erratum 2: zero terrain past a DEM tile edge. GLO-30 tiles declare no nodata value, so where a stack's grid needed two tiles, the mosaic kept 0 m beyond the first tile. Slope and HAND read as zero there, and shadow and layover were not flagged. The defect touched 172 of the 605 CEMS tiles (14.6 % of the benchmark's tile area), 6.4 % of Kuro Siwo's stack area and 8.6 % of Sen1Floods11's. Rebuilt with the fix, the CEMS tiles move the models that read terrain by +0.002 to +0.010 IoU and the others by at most 0.0001 (Table 2). The post-hoc reversal survives (−0.033 per activation, $p = 0.005$). Every v1.2 model is trained on rebuilt data and scored on rebuilt tiles.

Table 2: Erratum 2 on the CEMS benchmark: macro IoU at τ^* over 38 activations, on the original and the rebuilt tiles (`reports/v1_1_erratum.md`).

Model	Terrain	Original	Rebuilt	Change
Fusion (Kuro Siwo)	yes	0.3967	0.4070	+0.0103
Fusion (Sen1Floods11)	yes	0.2575	0.2658	+0.0083
Physics baseline	yes	0.3706	0.3725	+0.0019
SAR U-Net (Kuro Siwo)	no	0.3945	0.3946	+0.0001
SAR U-Net (Sen1Floods11)	no	0.2807	0.2808	+0.0001
TerraMind-small, corrected	no	0.2992	0.2992	+0.0000

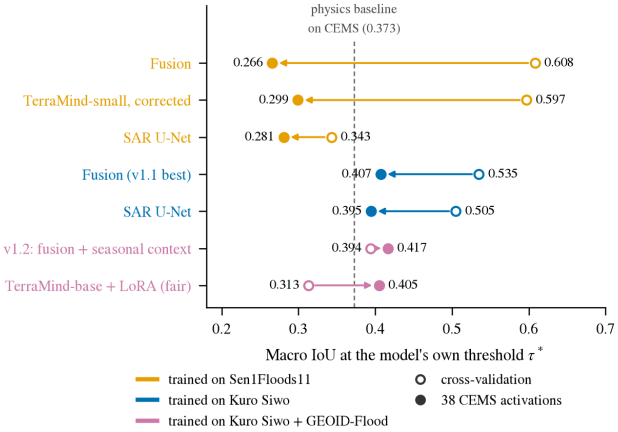


Figure 2: Each model's cross-validation score (open) beside its score on the 38 CEMS activations (filled). The cross-validation scores are chip-level macro IoU over held-out events or groups: three seeds for Sen1Floods11 and Kuro Siwo, one for the v1.2 pool. The CEMS scores are per-activation macro IoU, seeds pooled, on the rebuilt tiles. The two are not the same estimand; the size of the arrows is the point. Sources: `reports/v11_sen1floods11_table.md`, `v11_kurosiwo_table.md`, `v1_1_erratum.md`, `v12_pool_cv.md`, `v12_cems_rebuilt.json`.

5 Results

5.1 Cross-validation does not carry to independent maps

Figure 2 sets each model's cross-validation score beside its score on the 38 CEMS activations.

- **Sen1Floods11-trained models.** The optical models lose about half of their score or more: fusion falls from 0.608 in leave-one-event-out cross-validation to 0.266, and the corrected TerraMind-small from 0.597 to 0.299. The SAR U-Net falls less (0.343 to 0.281), because its cross-validation score was low to begin with. All three end below the physics baseline (0.373).
- **Grouping by event does not prevent this.** On Sen1Floods11, the published within-event split scored the fusion model between 0.03 lower and 0.06 higher than leave-one-event-out on the same test chips, depending on the seed, and none of these differences was significant after Holm. Both protocols sit far above the CEMS score.

The training data matter more. Trained on Kuro Siwo's flood labels, drawn on radar, the same architectures score 0.395 (SAR U-Net) and 0.407 (fusion) on CEMS. Their cross-validation scores (0.505 and 0.535) overstate them by 0.11 to 0.13 rather than by 0.3. v1.1's preregistered test of H1 compares two training recipes on identical Kuro Siwo chips that differ only in the label definition, which also changes the sampling, the early stopping and the calibration. Flood labels beat water labels by +0.059 IoU per activation (better on 33 of 38, Holm $p < 0.001$) and by +0.062 per cluster (27 of 30), on the original tiles. CEMS maps are themselves flood maps, so part of this gain is agreement of definitions. H1 is the only v1.1 hypothesis that was supported at both unit definitions and still stands. H4 was also supported as run, but its conclusion is withdrawn (Section 4.5). With the v1.2 pool, cross-validation no longer overstates the CEMS score: row 21 scores 0.394 in cross-validation and 0.417 on CEMS. The two numbers are different estimands (chips, one seed and 79 groups, against activations, three seeds and 38 units). We read them as the absence of a large bias, not as an exact match. Part of the agreement may also be shared conventions: GEOID-Flood's labels, which cover 102 of the pool's 138 floods, are themselves derived from CEMS delineations [6].

The optical input adds nothing detectable on independent maps.

- On Sen1Floods11, fusion beat the SAR U-Net by +0.265 on all ten events. Its labels were drawn on the Sentinel-2 image that the model sees.
- On the CEMS activations where optical was usable (≥ 50 % clear; v1.1 tiles), the gain was +0.038 $[-0.024, +0.108]$: not significant over eight activations (Holm $p = 0.344$), and no verdict, because seven clusters were too few.
- Under partial cloud (10–50 % clear, 15 activations, descriptive, v1.1 tiles), the Sen1Floods11-trained fusion model scored 0.254 with optical and 0.307 without.
- Trained on Kuro Siwo, the fusion model scores 0.397 with optical and 0.398 without (both on the v1.1 tiles).
- In the v1.2 pooled cross-validation, row 9 with optical minus row 9 without it at inference is −0.001 $[-0.011, +0.005]$.

5.2 v1.2 against the fair TerraMind in cross-validation

In pooled cross-validation, row 21 scores 0.394 at its own threshold and the fair TerraMind 0.313, a gap of 0.080 (Table 4). Most of it is threshold transfer. Each fold calibrates its threshold on the next fold's groups. Re-fitting each group's threshold on all the other groups (cross-fitting, from the stored counts, with no retraining) lifts TerraMind to 0.369 and leaves row 21 at 0.392: a gap of 0.023. At each group's best threshold the gap is 0.024 (0.430 vs 0.406). Threshold-free, row 21 leads by 0.034 AP (0.651 vs 0.617, fold-level). Row 9, the same model without the seasonal context, scores 0.383, and 0.382 cross-fitted. The seasonal context's edge over it is single-seed and modest.

5.3 On 38 CEMS activations: a near tie

The frozen models were scored once, after the freeze, on the rebuilt tiles (Table 3, Figure 3).

- **Row 21** scores 0.417 IoU at τ^* and 0.598 AP.
- **The fair TerraMind** scores 0.405 and 0.583.
- **v1.1's best model** scores 0.407 and 0.527.

Row 21 is better than TerraMind on 24 of the 38 activations (+0.012 IoU, +0.015 AP), and better than v1.1's best on 22 of 38 (+0.010). With the blind test's own analysis (Table 5), neither gap is significant.

Why the cross-validation gap shrank. Three observations bound the explanation.

(i) Threshold transfer accounted for most of the cross-validation gap (Section 5.2).

(ii) On CEMS, TerraMind's threshold transfers well. On the same binned per-seed scores, its IoU at τ^* (0.407) is 0.039 below its per-activation oracle (0.446), against 0.050 for row 21 (0.418 and 0.468).

(iii) The threshold-free gap also shrank, from 0.034 AP in cross-validation to 0.015 on CEMS.

The cross-validation comparison is single-seed and chip-level, the CEMS comparison three-seed and activation-level, and 38 activations resolve gaps of this size poorly. We therefore read the result as follows: on these maps, our task-specific model and the LoRA-adapted TerraMind-base are not distinguishable at this sample size (Holm $p = 0.37$). Both were trained and scored on data rebuilt with the DEM fix; TerraMind reads DEM gaps inside a window as 0 m (Section 8). The seasonal context's contribution on CEMS is not isolated, because no final model without it was scored there. Per-scene self-calibration barely helps row 21 (0.418 to 0.420 on the binned scores) and hurts TerraMind (0.407 to 0.362).

5.4 Copernicus GFM

On the 34 activations GFM covers, its ensemble flood extent scores 0.321 IoU, and its likelihood 0.517 AP. Every model we trained on flood labels scores above it: row 21 0.419, the fair TerraMind 0.400 and v1.1's best 0.407. So does the physics baseline, at 0.381, which uses no training labels. Only row 21's gap was tested. Row 21 is better on 25 of the 34 activations, by +0.098; per cluster the gap is +0.081 (17 of 26). The blind test's analysis code, applied to these seen floods, finds both gaps significant after Holm ($p = 0.0010$ and $p = 0.0185$). This is a descriptive result, not a test of H6.

Much of GFM's deficit lies in its fixed decision rule, exclusion mask included, rather than in how its likelihood ranks pixels. Thresholded at each activation's best value in hindsight, its likelihood reaches 0.427, 0.106 above its binary product. This oracle also re-admits pixels inside the exclusion mask, where the likelihood is defined but the binary product maps no flood. On its binned scores, row 21 gains 0.047 from the same oracle (0.420 to 0.467). Two features of GFM's design also work against it on this reference, and this study does not separate them:

- it maps no flood inside its exclusion mask, which includes dense vegetation and built-up areas;
- it is produced on a 20 m grid.

A sensitivity analysis restricted to GFM's non-excluded area was registered for the blind test on 13 November 2026, before any blind score is revealed; it is descriptive and has not been run on these seen floods. models may also benefit from

Table 3: Every model on the CEMS 2023–26 benchmark: primary stratum (products drawn on radar), EMSR664 excluded, units with reference flood, rebuilt tiles. IoU is the macro over units at each model's own τ^*, with a 95 % bootstrap interval over activations. The lower block restricts every model to the units GFM covers on at least 95 % of their scored pixels. GFM's binary product has no τ^*; its oracle IoU and AP come from its likelihood. All of this is exploratory: the benchmark was seen during development (`reports/v12_cems_rebuilt.md`).

		Per activation				Per cluster	
Model	Trained on	IoU at τ^* [95 % CI]	Self-cal.	Oracle	AP	IoU at τ^*	AP
All units: 38 activations, 30 clusters							
v1.2: fusion + seasonal context (row 21)	pool	**0.417** [0.365, 0.467]	**0.420**	**0.468**	**0.598**	**0.441**	**0.628**
TerraMind-base + LoRA, fair (row 24)	pool	0.405 [0.351, 0.455]	0.362	0.446	0.583	0.429	0.612
Fusion, v1.1's best (row 9)	Kuro Siwo	0.407 [0.355, 0.461]	0.407	0.438	0.527	0.431	0.553
SAR U-Net (row 4)	Kuro Siwo	0.395 [0.339, 0.448]	0.393	0.429	0.525	0.414	0.547
Physics baseline (row 2)	—	0.373 [0.314, 0.430]	—	—	—	0.405	—
TerraMind-small, corrected	Sen1Floods11	0.299 [0.250, 0.350]	0.303	0.356	0.428	0.312	0.445
SAR U-Net (row 4)	Sen1Floods11	0.281 [0.237, 0.322]	0.248	0.314	0.317	0.298	0.328
Fusion (row 9)	Sen1Floods11	0.266 [0.219, 0.317]	0.254	0.294	0.284	0.278	0.288
Units GFM covers: 34 activations, 26 clusters							
v1.2: fusion + seasonal context (row 21)	pool	**0.419** [0.363, 0.474]	**0.415**	**0.467**	**0.594**	**0.442**	**0.623**
TerraMind-base + LoRA, fair (row 24)	pool	0.400 [0.342, 0.457]	0.359	0.441	0.573	0.425	0.602
Fusion, v1.1's best (row 9)	Kuro Siwo	0.407 [0.346, 0.464]	0.405	0.437	0.523	0.429	0.545
Physics baseline (row 2)	—	0.381 [0.315, 0.443]	—	—	—	0.414	—
Copernicus GFM (ensemble)	—	0.321 [0.253, 0.387]	—	0.427	0.517	0.361	0.549

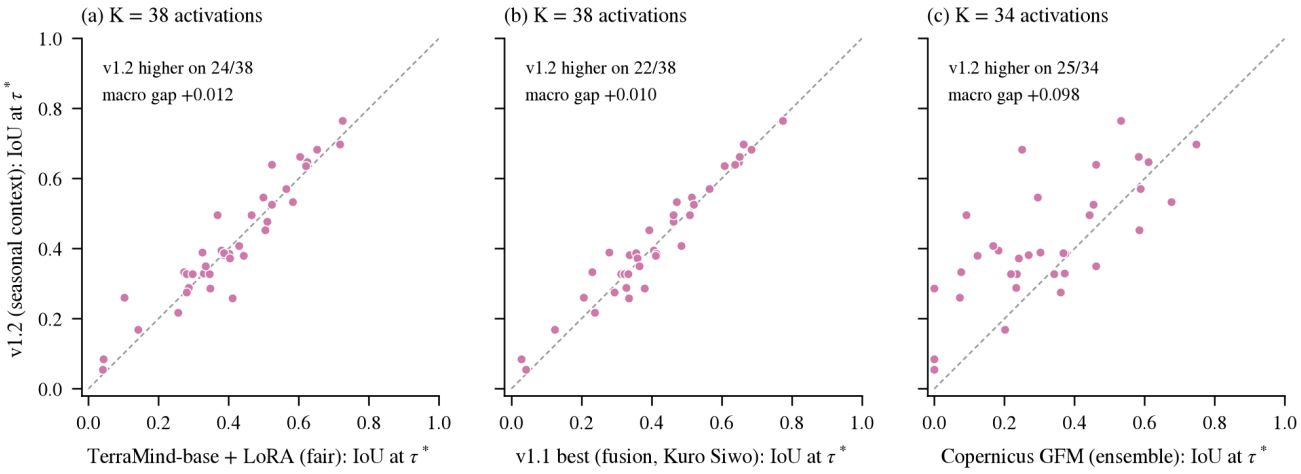


Figure 3: v1.2's model against (a) the fair TerraMind, (b) v1.1's best and (c) Copernicus GFM: one point per activation, IoU at each model's own threshold (GFM: its binary ensemble product), seeds pooled. Points above the diagonal favour v1.2. Panel (c) is restricted to the activations GFM covers. The counts and gaps match `reports/v12_cems_seen_tests.md`. Contains modified Copernicus Emergency Management Service information (2023–2026).

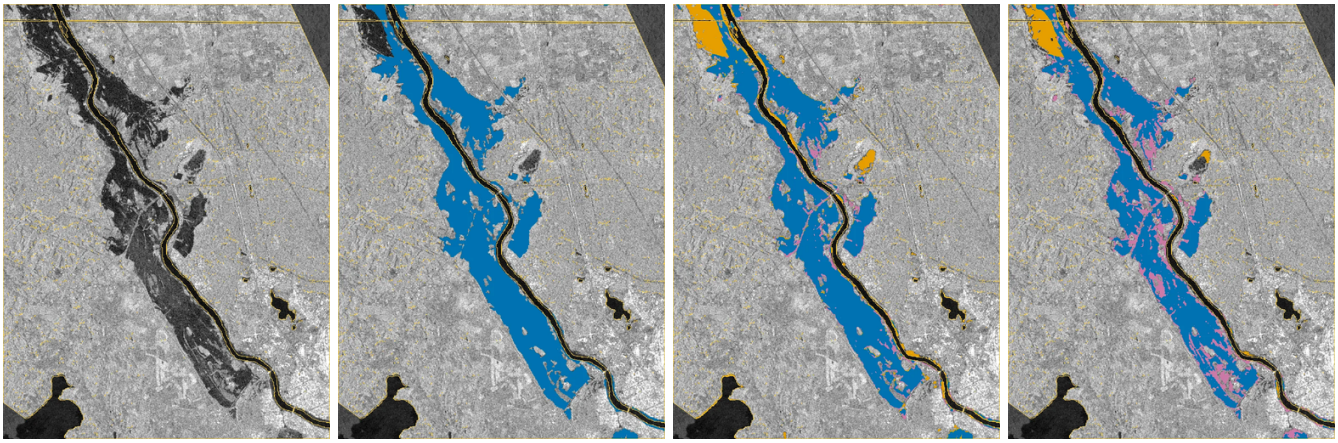
GEOID-Flood's CEMS-derived labels, which share the reference's mapping conventions; the physics baseline's lead over GFM shows that this does not explain the whole gap. Figure 4 shows one flood as the Arena renders it.

5.5 Consecutive Copernicus maps agree at 0.52

Over 79 pairs in 34 activations, consecutive CEMS delineations of the same area, made at most 24 h apart, agree at 0.520 macro IoU, and the median pair at 0.498 (Table 6). All 79 pairs are 6–24 h apart and none shares a source image. Pairs drawn on two radar images agree at 0.515. The sensitivity row leaves out EMSR657 AOI 1's three pairs, whose later products repeat 43–58 % of their flood from earlier images, and gives 0.509. Per activation, agreement ranges from 0.141 (EMSR841) to 0.987 (EMSR711).

By the reading fixed in the protocol, agreement near 0.5 places the benchmark near its ceiling: the models' 0.42 is close to the level at which the reference agrees with itself, rather than 0.42 of the way to a perfect map. The ceiling is not a bound, though: a model's map, compared under the same 24 h tolerance, can agree with one product better than the next product does. Nor is it two analysts mapping one image. It is the agreement of consecutive products, 6–24 h apart, so it mixes disagreement with real change in the flood, whereas the benchmark pairs each product with the Sentinel-1 pass nearest to it in time. The comparison with the models' scores is therefore indicative, not like for like.

Figure 5 pairs the two per activation, on the 27 activations in both sets, where the model scores 0.433 and the consecutive products agree at 0.536. The model scores below the reference's self-agreement in 20 of the 27, and the two are associated (Spearman $\rho = 0.51$, $p = 0.007$). This analysis was



(a) Sentinel-1 VV after the event **(b)** CEMS delineation (reference) **(c)** v1.1's best: tile IoU 0.761 **(d)** Copernicus GFM: tile IoU 0.690

Figure 4: One tile of EMSR657 (AOI 1, tile `t02_02`). The CEMS product was drawn on COSMO-SkyMed at 16:22 UTC on 8 April 2023; the Sentinel-1 pass was at 15:56 UTC; 24.81 km^2 of flood is mapped in the scored region. The quicklook shows Sentinel-1 VV from −25 to 0 dB. Inside the scored region (yellow outline) the colours are **hit**, **false alarm** and **miss**; outside it the radar is dimmed. The Arena's quicklooks were rendered before the freeze, so they show the v1.1 models (seed 42) and GFM, not v1.2's model; the tile IoU is not the activation's macro score. Contains modified Copernicus Sentinel data (2023) and modified Copernicus Emergency Management Service information (2023), © European Union.

Table 4: Pooled grouped five-fold cross-validation, chip level, one seed, 81 groups (79 with a defined IoU). "Cross-fitted": each group's threshold fitted on the other groups' held-out predictions. "Best": each group's best threshold in hindsight. AP is fold-level. The last row is derived from the unrounded values. Source: `reports/v12_pool_cv.md`.

	IoU at threshold			
Model	own τ^*	cross-fitted	best	AP
Row 21 (seasonal context)	0.394	0.392	0.430	0.651
Row 9 (no context)	0.383	0.382	0.425	0.632
TerraMind-base + LoRA	0.313	0.369	0.406	0.617
Row 21 − TerraMind	0.080	0.023	0.024	0.034

Table 5: The blind test's analysis (`floodfusion.blind_analysis`), unchanged, applied to the seen CEMS floods. "B > A": units where v1.2 is better. This is descriptive, not the preregistered test (`reports/v12_cems_seen_tests.md`).

Test (v1.2 − A)	Unit	K	Gap	B > A	AP gap	Holm p
P5: fair TerraMind	activ.	38	+0.012	24	+0.015	0.3663
	cluster	30	+0.012	19	+0.016	0.3293
P6: GFM	activ.	34	+0.098	25	—	0.0010
	cluster	26	+0.081	17	—	0.0185
P7: v1.1's best	activ.	38	+0.010	22	—	0.3663
	cluster	30	+0.010	18	—	0.3293

Had these been the blind floods, P5 and P7 would read *not supported* and P6 *supported*.

chosen after both had been computed, and it is exploratory. It is what one would see if floods that analysts cannot delineate consistently are also hard for a model; it is also what one would see if both depend on a third property, such as the flood's size or how fast it changes.

5.6 Adapting to Copernicus's own labels

Neither rung was adopted (Table 7). R1, row 21's seed 42 scored fold by fold, gives 0.421; the three seeds pooled give 0.417 (Table 3).

R2: a threshold refitted on other CEMS floods. It gains +0.002 and is better on 26 of 38 activations, so it fails the 0.005 gain the rule asks for. The fold thresholds range from 0.237 to 0.331, around $\tau^* = 0.25$. With seeds 43 and 44, R2 would gain +0.014 and +0.010 (descriptive; the rule fixed seed 42). A threshold learned from other CEMS floods may therefore help a little, but nowhere near the 0.05 that each activation's own best threshold leaves (Section 5.3): the best threshold varies between floods more than between our training pool and CEMS.

R3: fine-tuning on CEMS labels. It scores 0.380 against R1's 0.421: −0.041, better on 15 of 38 activations and on 12 of 30 clusters. It is not adopted, so there is no v1.3 model and H8 is not run. Part of the loss is in the ranking itself: AP falls from 0.606 to 0.573, and the oracle IoU from 0.468 to 0.457. Most of the loss at τ^*, though, is calibration: R3 sits 0.077 below its oracle IoU and R1 0.047, and each fold fits R3's calibration on its validation groups alone (protocol v1.3 §3). +0.131 (EMSR841) to −0.336 (EMSR771), with a median of −0.014 (Figure 6).

- **Two folds carry the loss.** Fold 0 (nine activations) falls from 0.367 to 0.270 and fold 1 (seven) from 0.401 to 0.297, better on 2 and on 0 of their activations. The other three folds change by +0.016, −0.011 and +0.004.
- **Training length does not separate them.** Fold 1's model scored best on its validation fold after the first epoch, fold 0's after the 28th; both lost.
- **Optical products.** On the six activations whose products were drawn on optical images, R3 scores 0.163 and R1 0.158.

The tuning and the five fold models took 9.2 GPU-hours, below the 20–28 estimated, because early stopping ended four of the five folds well before 30 epochs.

Table 6: The reference ceiling: IoU between two CEMS delineations of the same area, made at most 24 h apart, seen flood activations only; descriptive (`reports/reference_ceiling.md`). All 79 pairs are 6–24 h apart and none shares a source image. Sensitivity: without the pairs whose later product repeats more than 5 % of its flood.

Pairs	Activ.	Pairs	Macro IoU	Median pair
All	34	79	**0.520**	0.498
Sensitivity	33	76	0.509	0.491
Radar–radar	32	75	0.515	0.502
Radar–optical	2	2	0.380	0.380
Optical–optical	1	1	0.796	0.796
Other	1	1	0.329	0.329

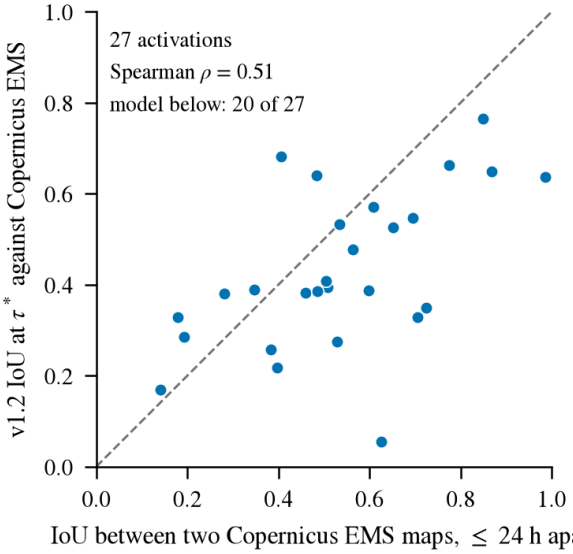


Figure 5: Per seen activation: v1.2's model (row 21) at τ^* against CEMS (y), and the IoU between two CEMS delineations of the same area at most 24 h apart (x), on the 27 activations in both sets. Dashed: equal agreement. Exploratory: chosen after both were known (`paper/igarss27/figures/ceiling_scatter.json`). Contains modified Copernicus Emergency Management Service information (2023–2026).

6 The preregistered blind test

The CEMS 2023–26 benchmark cannot settle v1.2's questions. It was v1.1's test set, it was seen during v1.2's development, and public training sets now cover its activations. Because it was seen, the protocol, committed on 13 October 2026 before any v1.2 model was trained, makes only the blind test confirmatory. Before the freeze, a preview (14 October, after H6 had been registered) scored GFM and the v1.1 models on that benchmark (`reports/v12_cems_preview.md`); v1.2's final models were scored on it only after the freeze.

6.1 Hypotheses and tests

Each hypothesis compares B, v1.2's model (row 21), with an opponent A, on the primary stratum, at two unit definitions:

- **H5 (P5):** B beats the fair TerraMind, both at each model's own threshold and threshold-free.
- **H6 (P6):** B beats Copernicus GFM, on the units GFM covers.
- **H7 (P7):** B beats v1.1's best model.

Statistic and test. The statistic is the per-unit gap B − A in macro IoU at τ^*, seeds pooled. Each test is an exact two-sided sign-flip test, Holm-adjusted across P5–P7 within each unit definition. The family always has three members: a test with fewer than eight units enters it with $p = 1$.

P5 needs more. The same must also hold for AP. Its two conditions form one intersection–union test, $p = \max(p_{\text{IoU}}, p_{\text{AP}})$. This closes a loophole of v1.1, where a win at τ^* reversed at the oracle threshold. The condition was written on 13 October, before any v1.2 cross-validation run.

Verdicts. A hypothesis is *supported* if its test is significant with a positive gap at both unit definitions, and *refuted* if it is significant with a negative gap at both. Below eight units at either definition it has *no verdict*; otherwise it is *not supported*.

H8, registered later and not run. v1.3's protocol registered H8: v1.3's model beats v1.2's on the blind floods, with the same metric, test and units, tested alone at $\alpha = 0.05$ because it cannot join the frozen family of three. It was to be run only if the ladder adopted a rung. It adopted none (Section 5.6), so H8 is not run and the blind test keeps P5–P7 as

Table 7: The adaptation ladder on the 38 seen activations, cross-validated, seed 42 (`reports/v13_ladder.md`). "Better": activations where the rung beats R1. Rule: a gain of at least 0.005 and better on more than half. Clusters, AP and the oracle IoU are descriptive; R2 changes only the threshold, so its AP and oracle IoU are R1's.

Rung	IoU	Cluster	Better	AP	Oracle	Verdict
R1, zero-shot	0.421	0.444	—	0.606	0.468	base
R2, refitted τ	0.423	0.446	26	= R1	= R1	not adopted
R3, fine-tuned	0.380	0.403	15	0.573	0.457	not adopted

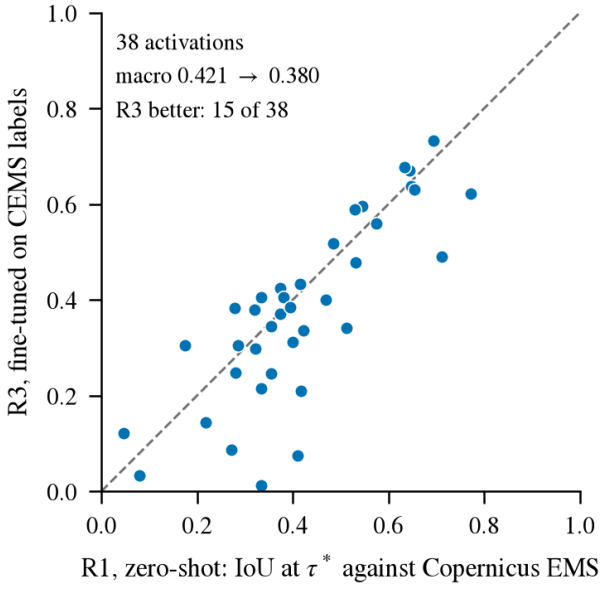


Figure 6: Per activation, cross-validated: the zero-shot model (R1, x) against the same model fine-tuned on the other folds' CEMS labels (R3, y), both at τ^*. Dashed: no change. Seed 42 (`paper/igarss27/figures/ladder_r3.json`). Contains modified Copernicus Emergency Management Service information (2023–2026).

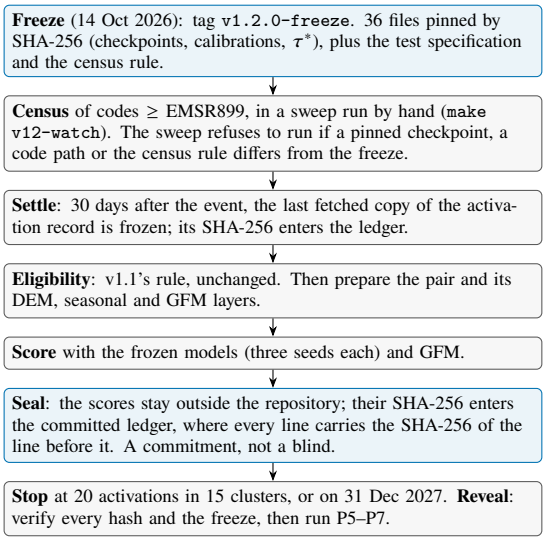


Figure 7: The blind test's pipeline (`floodfusion.prospective`). The ledger is append-only and hash-chained: against its committed history, an edited, removed or reordered line is detectable.

frozen.

6.2 The blind set

The blind set is every Copernicus EMS flood activation with code EMSR899 or above, put through v1.1's eligibility rule unchanged, at most four AOIs per activation. The first activations in that range date from 20 July 2026. The first three blind flood activations (events on 21 August, 25 August and 1 October 2026) predate the freeze of 14 October, and the fourth (19 October) followed it. They are blind in a precise sense:

- no model was trained or tuned on them;
- none was looked at during development;
- every one is scored only after the freeze.

Only metadata was seen. On 13 October the code, date, category and name of EMSR899–945 were queried to estimate accrual, and this is disclosed in the protocol. During this paper's fact-check, a reviewing agent also read the cached activation record of EMSR933: its product list and their statuses, no map, pass or score. This too is logged in the deviations log. The training activations all precede EMSR656 (2023), and TerraMind's pre-training data date mostly from 2019–2023. GFM itself is not frozen: the test uses whatever version EODC serves, and records it, and GFM's ensemble members change in 2027.

6.3 Freeze, sealing and the ledger

The freeze tag pins the models and their calibrations: 36 files are listed by SHA-256 in `reports/v12_freeze.json`. Figure 7 shows the pipeline. Before any blind flood was scored, the whole runner was rehearsed on EMSR664, which lies outside the blind set: one pair, eight tiles, scored by every frozen model and GFM, sealed and verified against a scratch ledger in 15 minutes.

The seal is a commitment, not a blind. The sealed files are plain JSON on the author's machine, so the seal makes later changes detectable but does not hide the scores. Sweeps are run by hand, and the runner freezes the last record it fetched before an activation settles. A sweep should therefore run shortly before each settle time, or products published late may be missed.

Table 8: Smallest true mean IoU gap that the blind test detects at 80 % power at Holm's smallest level (0.0167), by number of activations (`reports/v12_power.md`).

Per-activation spread (v1.1)	10	15	20	30
SD 0.077 (P4)	0.096	0.072	0.061	0.048
SD 0.071 (P3)	0.089	0.066	0.056	0.044

6.4 Power and stopping

The stopping rule was raised, before any blind flood was looked at, from 10 activations in 8 clusters to 20 in 15. Table 8 gives the reason. Gaps are simulated as i.i.d. normal with v1.1's per-activation spread, which omits clustering. At Holm's smallest level for three tests (0.05/3), 20 activations detect a mean gap of 0.061 IoU at 80 % power, and 10 would detect only 0.096. A verdict needs significance at both unit definitions, and 15 clusters detect 0.072; P5 also needs AP. The end date may come before the counts are reached, with lower power. The gaps seen on CEMS for P5 and P7 (about 0.01) are far below these. Unless new floods behave differently, P5 and P7 will most likely end *not supported*. P6's seen gap (0.098) lies above it.

6.5 Status

Two sweeps have run, on 14 October and 11 November 2026. The first took the census to EMSR934. The ledger reads:

- EMSR926 (Latvia and Lithuania) and EMSR927 (Nepal): not eligible under v1.1's rule;
- EMSR933 (Crete, event on 1 October): one AOI (AOI 4) scored and sealed. Its product was drawn on optical images, so it lies outside the primary stratum on which P5–P7 are tested;
- EMSR935 (event on 19 October): settling, judged after 18 November.

No activation of the primary stratum has been scored yet.

A lapse. No sweep ran between 14 October and 11 November, and EMSR933 settled on 31 October without one. The frozen runner never fetches a settled activation's record again, so EMSR933 was judged on its record as cached on 14 October: products published later were not seen. The lapse was logged before the second sweep. The cached record was left as it was, because deleting it to force a new fetch would have been a hand intervention in the blind test's state. From release v1.3.0, a scheduled job opens a reminder issue on the repository when the ledger's newest row is a week old; it reads the committed ledger and nothing else, so it touches no blind flood.

The Arena shows only counts and statuses until the stopping rule is met.

7 The frozen model in service

A model frozen for a blind test can still be used. v1.3 publishes it and runs it on Sentinel-1 passes, under rules that keep

the blind test intact.

Weights. Row 21's three frozen seeds are published on Hugging Face Hub under CC BY 4.0, the licence of their training labels: byte for byte the checkpoints, run records and calibrations that the freeze manifest pins, with a `SHA256SUMS` file. The downloader fetches them at a pinned revision and checks every file against the freeze manifest before it is used. No weights trained on Sen1Floods11, which declares no licence, are published.

A map of any place and date. One command (`python -m floodfusion.live map`, with a box and a date) finds the Sentinel-1 pass of that date and builds the benchmark's input stack without a label: the same-orbit pre-event pass, the seasonal reference, the DEM and its derivatives, JRC water, WorldCover, and Sentinel-2 within ±2 days where it is clear. It runs the frozen model on CPU and writes, per tile, cloud-optimised GeoTIFF layers, a STAC item and flood polygons, with the exclusion mask and a low-confidence band.

Does a live map rebuild the benchmark? We replayed one seen tile (EMSR683 AOI 2, Norway, 10 August 2023). The live stack's grid and all 14 of its input bands were identical to the benchmark's, pixel for pixel, and its seasonal reference came from the same five scenes. On the benchmark's stack, a CPU run gives the stored GPU run's IoU at τ^* (0.4141). On the live stack, the same pixels score 0.4210. The live stack has no area of interest, so the model also reads the ground around it, and its receptive field carries that context inside. A live map is therefore not the benchmark's prediction of the same pixels, and the service never reports a score.

The watcher. A scheduled job (GitHub Actions, every six hours) chooses the next maps and publishes their polygons, STAC items and an index on a data branch, which the project's live page reads. It makes at most two maps per run, because a tile takes about a minute on four CPU threads. It maps a showcase of seen activations, each AOI on every pass from the event date to three days after, and manual requests. It also watches every new flood activation for 30 days after its event and maps each new pass over at most four of its AOIs.

What it may read and show. The service reads only an activation's code, name, category, event date and AOI extents, never a CEMS product, and the live page shows no Copernicus outline and no score for any flood. Blind floods were held back by a rule logged before the service ran. While a committed switch was off, the service refused every code from EMSR899 on before it requested the record, and any date whose optical window reaches 20 July 2026, the first event date of the blind set, so that a map of an arbitrary box could not show a blind flood either; tests enforce both. By v1.3's protocol the switch could be turned on only after the v1.3 freeze, or after the ladder had decided that there is no v1.3 model, and only on the author's go. The ladder decided on 11 November 2026, and the author switched blind floods on on 13 November, logged before the first map of one existed. Showing a blind flood's map cannot change its score: the models are frozen, and every blind score is computed only by the blind test's runner and committed to its ledger. The rule protected the development of a later model, which must not see blind outputs before it is frozen; with no v1.3 model, none is in development. Once shown, though, the blind floods can no longer serve as unseen test data for a model developed after the switch. The service is a research demonstration, not an operational or official Copernicus product.

8 Discussion

What moved the scores.

- **The training data, labels included**: 0.141 IoU on CEMS between the same fusion model trained on Sen1Floods11 and on Kuro Siwo;
- **the threshold**: most of a 0.080 gap in cross-validation; on CEMS the two v1.2 models lose 0.039 and 0.050 IoU against their oracle thresholds;
- **the system**: 0.012 on CEMS between our model and the fair TerraMind, with encoder, inputs and context together;
- **the optical input**: about zero;
- **adapting to the reference**: +0.002 from a threshold refitted on other CEMS floods, and −0.041 from fine-tuning on their labels.

As in GEOID-Flood [6] and PANGAEA [11], the choice of encoder moved scores little; unlike GEOID-Flood, we see no foundation-model advantage. For operational use, labels with flood semantics and an explicit decision rule mattered more here than the network.

Reading a score against its reference. A score of 0.42 IoU against CEMS reads differently beside the reference's own agreement: two consecutive CEMS maps of one area, hours apart, agree at 0.52. On the 27 activations in both sets, the model scores 0.433 and the consecutive products agree at 0.536, a gap of about 0.1 IoU. Part of the model's shortfall is the threshold: over the 38 activations, each activation's best threshold in hindsight lifts it from 0.417 to 0.468, which neither our calibration nor a threshold refitted on other floods recovers. Benchmarks that score models against analyst maps could report the reference's self-agreement beside every score, as other fields report agreement between annotators. Without it, a reader cannot tell how much of a score's distance from 1 is the model's.

Why adapting to the reference did not help. We did not test an explanation, but three observations bound one.

- **The labels already carried CEMS's conventions.** GEOID-Flood's labels, 102 of the pool's 138 floods, are derived from CEMS delineations [6], so fine-tuning added few new conventions.
- **The reference is inconsistent.** If two maps of one flood agree at 0.52, a model fitted to a few dozen activations' maps can learn their particular conventions rather than flood. The change varied between floods, from +0.13 to −0.34.
- **There were few floods.** Each fold model trains on three of five folds of 43 activations, against the pool's 138 floods, and one seed decides each rung.

A model trained on CEMS labels from the start, on more activations, might behave differently; the ladder tested adaptation of a model that was already good on this reference, under a rule that asked for a clear gain.

What a fair comparison needs. A fair comparison needs five things:

- the same labels and data;

- the same training recipe;
- the same tuning budget;
- each model's native inputs;
- rules fixed before results.

It also needs a threshold-free metric beside the thresholded one, because thresholds transfer differently from one model to another. Our TerraMind opponent (row 24) met the first, second and fifth. Its tuning budget covered only the learning rate, and its inputs were not fully native (Limitations), so "fair" in its name states the intent of the design, not a guarantee. Our v1.1 comparison failed the recipe condition through a bug (erratum 1). It was caught while preparing a fair opponent for v1.2.

Reading the GFM comparison. GFM is built for automated global operation, with conservative exclusions and one decision rule for every scene. Its likelihood ranks pixels reasonably (AP 0.517). A threshold chosen for each activation in hindsight would lift it to 0.427, but no such threshold is available in operation. A per-scene recalibration of our own models did not help in cross-validation either (−0.042 for row 21). Adapting a decision rule to each scene is not free.

Limitations.

- **Reference maps are products, not ground truth.** CEMS delineations are generalised analyst maps, drawn on commercial images (34 of the 75 primary pairs on VHR2-class images, 41 on coarser HR+-class images) taken up to 24 h from the Sentinel-1 pass. Low IoU partly measures the difference between two products.
- **Consecutive-product agreement.** Its 0.520 includes real change in the flood within 24 h, which lowers it, while an analyst who starts a product from the previous one raises it; the carry-over probe found that only in EMSR657 AOI 1. It is not the agreement of two analysts on one image. It covers the 34 activations mapped twice within a day, which may differ from those mapped once, and only 27 of them are among the 38 the models are scored on.
- **The ladder.** One seed decides each rung, on 38 seen activations. R2's verdict depends on the seed: with seeds 43 and 44 it would gain more than 0.005. Fine-tuning used one recipe, row 21's, and one of three learning rates; it does not show that no adaptation could help.
- **The benchmark is seen and small.** The CEMS 2023–26 benchmark informed development, and 38 activations resolve gaps of about 0.01 poorly. GEOID-Flood's labels are themselves derived from CEMS delineations. The cross-validation is single-seed.
- **The opponent's configuration.** The size rule, fixed for the 8 GB GPU, stopped at TerraMind-base; TerraMind-large was not tried. LoRA adapts only the attention projections. TerraMind's SAR input is our z-scored backscatter, adapted by four affine parameters rather than its pre-training normalisation. The band subset and necks follow IBM's Sen1Floods11 recipe, and the schedule is row 9's. The equal tuning budget covers only the learning rate, whereas row 9's design went through two earlier releases. Missing DEM pixels inside an available window read as 0 m (disclosed before the freeze).
- **Pre-training exposure.** TerraMind's pre-training data date mostly from 2019–2023, so its encoder may have seen unlabelled imagery of the benchmark's 2023 events; "never saw the event" holds for its decoder.
- **The selection.** The inner validation groups used for tuning serve as test groups in other folds. This applies to both families equally, by design.
- **GFM.** The effects of GFM's exclusion mask and its 20 m grid are not separated. GFM versions are mixed on the benchmark, and GFM is not frozen for the blind test.
- **Overlap.** Place overlap between the v1.2 pool and the benchmark was not re-measured. v1.1 found five pairs overlapping Kuro Siwo training areas, and dropping them left H1's verdict unchanged.
- **Training data defects.** The v1.1 models were trained on data that carried erratum 2 and were not retrained.
- **Timestamps.** Commit dates are set by the author's machine. GitHub first received the protocol and the freeze tag on 15 October 2026, before any blind flood was scored. Software Heritage archived the repository, the protocol, the freeze tag and the ledger included, on 13 November 2026 (`swh:1:snp:084feda8e19a3768ad891541e25a8e6d74f8421f`). That is after the first blind AOI was scored, on 11 November, so the archive fixes the freeze's content from then on, not its date. Zenodo archived release `v1.3.0` the same day (doi:10.5281/zenodo.24194785).

9 AI-assisted engineering and reproducibility

Provenance and the author's role. The author, Teo Clerici Jurado, wrote the original v1.0 project specification and defined the project's core research objectives: to test findings made on Sen1Floods11 against real Copernicus EMS activations, to audit whether the comparison with a foundation model, TerraMind, is fair, and to decide the main comparison by a preregistered blind test. The specification fixed v1.0's architecture, its ablation grid, the training recipe and the decision rule. The repository's first commit (`212e0e6`, 9 October 2026) imported it unchanged (the meaning of "as received" in its message) with a skeleton package, the ablation configurations and a test specification of 281 test functions. The specification documents were removed from the history before publication and are not public; the commit holds the package, the configurations and the tests. The author directed the agent workflow described below: they set each release's goals, reviewed and approved each release's plan, and made the decisions on data licensing, compute scheduling and publication. The v1.2 protocol, preregistration design included, was drafted with Claude Code and reviewed and approved by the author; the audits were run by AI subagents. For v1.3 the author chose its aims (a live service, a model adapted to Copernicus's labels, and a paper), chose to train the ladder on every stratum, and decided which weights to publish and under which licence; the v1.3 protocol was drafted with Claude Code and approved by the author before any of its results existed. The author takes full scientific responsibility for the work, its errata and corrections, and this paper.

Use of an AI coding agent. The project was built with Claude Code (Anthropic), an AI coding agent that the author operated throughout. In line with the generative-AI policies

of IEEE and AGU, and of venues such as NeurIPS, the agent is not an author, its use is described here, and the human author is accountable for the results. Under the author's direction, the agent:

(i) searched and summarised the literature, and drafted the v1.2 study design, the protocol text and the analysis rules, which the author approved;
(ii) implemented the specification and the later releases: the data pipeline, the models, the scorers, the blind-test runner, the Arena page and the live service;
(iii) extended the test suite from the 281 specified test functions to 976, which parametrisation expands to 1,240 test cases;
(iv) ran structured review passes with separate agent instances: code, Python, machine-learning engineering and security. Their findings were fixed or, where a fix would have changed models already cross-validated, disclosed; findings that touched a rule were logged before the result they could affect. The review of the blind-test design checked for train–test leakage and found none. These reviewers are instances of the same AI system that wrote the code, so they are not independent of it;
(v) traced and measured both errata;
(vi) fact-checked the documentation, and this manuscript, against the generated reports;
(vii) drafted this manuscript.

The deviations logs record each rule before the result it could affect, and disclose the exceptions: for example, v1.1's first amendment was written after the Stage A diagnostics of the v1.0 models.

Reproducibility.

- **Runs and reports.** Every training run records its code commit, whether the tree was clean, and hashes of its configuration, manifest and splits. The table builders refuse runs made from different code, mixed data sets or mixed test sets.
- **Environment and tests.** The environment is locked with uv. Continuous integration runs the linter and the offline test suite on Python 3.11 and 3.12. At this release, 1,238 offline tests pass and 2 are skipped, with 82.7 % combined statement and branch coverage of the package; tests that need live services are excluded by default.
- **The blind test.** Its models, calibrations, thresholds and specification are pinned by SHA-256 at the freeze tag, and the published weights are checked against the same manifest.
- **Compute.** Every experiment ran on one laptop GPU (NVIDIA RTX 4060 Laptop, 8 GB), one job at a time; v1.3's ladder took 9.2 GPU-hours. The live service runs on CPU.

10 Conclusion

On the seen CEMS benchmark (exploratory), the training data and the decision rule mattered more than the network:

- a task-specific seasonal-context model and a LoRA-adapted TerraMind-base are not distinguishable over 38 activations;
- both score above GFM's binary product on the floods it covers (0.419 and 0.400 against 0.321; only the first gap was tested);
- from cross-validation on a benchmark whose labels share the model's inputs to independent maps, a model's score fell by up to 0.34 IoU, a drop that mixes optimistic cross-validation with a change of label (water against flood);
- the reference agrees with itself at 0.520, so scores near 0.42 should be read against that level, not against 1;
- neither a threshold refitted on other CEMS floods nor fine-tuning on their labels closed the gap, under a rule fixed in advance.

The decisive comparison is the blind test. Frozen models, hash-committed scores and a fixed stopping rule will decide H5–H7 on floods that none of the models had seen. Meanwhile the frozen model is public, and its service maps floods from Sentinel-1 in the open.

Data and code availability

The code (MIT licence), the protocols, the deviations logs and every report are at `https://github.com/teo-clerk/floodfusion`. The release is tag `v1.3.0`, archived on Zenodo (`https://doi.org/10.5281/zenodo.24194785`) and Software Heritage, and the blind test's models are frozen at tag `v1.2.0-freeze`. The frozen weights of v1.2's model (row 21, three seeds) are at `https://huggingface.co/teo-clerk/floodfusion` under CC BY 4.0, at revision `faed3bb78668cf25052211a7e834f34652a4cdf6`. The interactive Arena (`https://teo-clerk.github.io/floodfusion/arena.html`) shows every model on the same floods, and the live page (`https://teo-clerk.github.io/floodfusion/live.html`) the service's maps. Every input comes from public sources and needs no credentials: Microsoft Planetary Computer, the CEMS rapid-mapping API, EODC's GFM catalogue, the Kuro Siwo annotations and GEOID-Flood. Sen1Floods11 declares no licence, so its data, chips and the weights trained on it are not redistributed. Kuro Siwo (CC BY) and GEOID-Flood (CC BY 4.0) are re-downloaded by the user rather than redistributed.

Acknowledgements

Contains modified Copernicus Sentinel data (2015–2026), accessed through Microsoft Planetary Computer; Sentinel-1 RTC processed by Catalyst (CC BY 4.0). Contains modified Copernicus Emergency Management Service information (2023–2026): rapid-mapping delineations and Global Flood Monitoring (GFM) flood maps, © European Union. Copernicus DEM © DLR e.V. 2010–2014 and © Airbus Defence and Space GmbH 2014–2018, provided under COPERNICUS by the European Union and ESA. JRC Global Surface Water: EC JRC/Google. ESA WorldCover 2021. TerraMind: IBM and ESA. Kuro Siwo: Orion AI Lab, data CC BY, annotation code MIT. GEOID-Flood: Chiriaco et al., CC BY 4.0. The weights are hosted by Hugging Face. Claude Code (Anthropic) was used to implement the software and to draft this manuscript; Section 9 describes its use.

References

[1] Copernicus Emergency Management Service. Rapid mapping: activations and products. https://rapidmapping.emergency.copernicus.eu/, 2026. Accessed 2026-10-15.

[2] Peter Salamon, Niall McCormick, Christopher Reimer, Tom Clarke, Bernhard Bauer-Marschallinger, Wolfgang Wagner, Sandro Martinis, Candace Chow, Christian Böhnke, Patrick Matgen, Marco Chini, Renaud Hostache, Luca Molini, Elisabetta Fiori, and Andreas Walli. The new, systematic global flood monitoring product of the Copernicus emergency management service. In *2021 IEEE International Geoscience and Remote Sensing Symposium (IGARSS)*, pages 1053–1056, 2021. doi: 10.1109/IGARSS47720.2021.9554214.

[3] Christian Krullikowski, Candace Chow, Marc Wieland, Sandro Martinis, Bernhard Bauer-Marschallinger, Florian Roth, Patrick Matgen, Marco Chini, Renaud Hostache, Yu Li, and Peter Salamon. Estimating ensemble likelihoods for the Sentinel-1-based global flood monitoring product of the Copernicus emergency management service. *IEEE Journal of Selected Topics in Applied Earth Observations and Remote Sensing*, 16:6917–6930, 2023. doi: 10.1109/JSTARS.2023.3292350.

[4] Derrick Bonafilia, Beth Tellman, Tyler Anderson, and Erica Issenberg. Sen1Floods11: A georeferenced dataset to train and test deep learning flood algorithms for Sentinel-1. In *2020 IEEE/CVF Conference on Computer Vision and Pattern Recognition Workshops (CVPRW)*, pages 835–845, 2020. doi: 10.1109/CVPRW50498.2020.00113.

[5] Nikolaos Ioannis Bountos, Maria Sdraka, Angelos Zavras, Ilektra Karasante, Andreas Karavias, Themistocles Herekakis, Angeliki Thanasou, Dimitrios Michail, and Ioannis Papoutsis. Kuro Siwo: 33 billion m^2 under the water. A global multi-temporal satellite dataset for rapid flood mapping. In *Advances in Neural Information Processing Systems 37 (Datasets and Benchmarks Track)*, pages 38105–38121, 2024.

[6] Gaetano Chiriaco, Luca Barco, Andrea Bragagnolo, Claudio Rossi, and Edoardo Arnaudo. GEOID-Flood: A large-scale multi-modal benchmark dataset for flood segmentation. arXiv:2608.02315, 2026. ECCV 2026 Terrabytes II Workshop.

[7] Johannes Jakubik, Felix Yang, Benedikt Blumenstiel, Erik Scheurer, Rocco Sedona, Stefano Maurogiovanni, Jente Bosmans, Nikolaos Dionelis, Valerio Marsocci, Niklas Kopp, Rahul Ramachandran, Paolo Fraccaro, Thomas Brunschwiler, Gabriele Cavallaro, Juan Bernabe-Moreno, and Nicolas Longépé. TerraMind: Large-scale generative multimodality for earth observation. arXiv:2504.11171, 2025. ICCV 2025.

[8] David R. Roberts, Volker Bahn, Simone Ciuti, Mark S. Boyce, Jane Elith, Gurutzeta Guillera-Arroita, Severin Hauenstein, José J. Lahoz-Monfort, Boris Schröder, Wilfried Thuiller, David I. Warton, Brendan A. Wintle, Florian Hartig, and Carsten F. Dormann. Cross-validation strategies for data with temporal, spatial, hierarchical, or phylogenetic structure. *Ecography*, 40(8):913–929, 2017. doi: 10.1111/ecog.02881.

[9] Pierre Ploton, Frédéric Mortier, Maxime Réjou-Méchain, Nicolas Barbier, Nicolas Picard, Vivien Rossi, Carsten Dormann, Guillaume Cornu, Gaëlle Viennois, Nicolas Bayol, Alexei Lyapustin, Sylvie Gourlet-Fleury, and Raphaël Pélissier. Spatial validation reveals poor predictive performance of large-scale ecological mapping models. *Nature Communications*, 11:4540, 2020. doi: 10.1038/s41467-020-18321-y.

[10] Hanna Meyer and Edzer Pebesma. Machine learning-based global maps of ecological variables and the challenge of assessing them. *Nature Communications*, 13:2208, 2022. doi: 10.1038/s41467-022-29838-9.

[11] Valerio Marsocci, Yuru Jia, Georges Le Bellier, David Kerekes, Liang Zeng, Sebastian Hafner, Sebastian Gerard, Eric Brune, Ritu Yadav, Ali Shibli, Heng Fang, Yifang Ban, Maarten Vergauwen, Nicolas Audebert, and Andrea Nascetti. PANGAEA: A global and inclusive benchmark for geospatial foundation models. arXiv:2412.04204, 2024.

[12] Mirela G. Tulbure, Julio Caineta, Mark Broich, Mollie D. Gaines, Philippe Rufin, Leon-Friedrich Thomas, Hamed Alemohammad, Jan Hemmerling, and Patrick Hostert. Leveraging AI multimodal geospatial foundation models for improved near-real-time flood mapping at a global scale. arXiv:2512.02055, 2025.

[13] A. D. Nobre, L. A. Cuartas, M. Hodnett, C. D. Rennó, G. Rodrigues, A. Silveira, M. Waterloo, and S. Saleska. Height above the nearest drainage – a hydrologically relevant new terrain model. *Journal of Hydrology*, 404(1–2):13–29, 2011. doi: 10.1016/j.jhydrol.2011.03.051.

[14] Carlos Gomes, Benedikt Blumenstiel, Joao Lucas de Sousa Almeida, Pedro Henrique de Oliveira, Paolo Fraccaro, Francesc Marti Escofet, Daniela Szwarcman, Naomi Simumba, Romeo Kienzler, and Bianca Zadrozny. TerraTorch: The geospatial foundation models toolkit. arXiv:2503.20563, 2025. IGARSS 2025.

[15] Edward J. Hu, Yelong Shen, Phillip Wallis, Zeyuan Allen-Zhu, Yuanzhi Li, Shean Wang, Lu Wang, and Weizhu Chen. LoRA: Low-rank adaptation of large language models. In *International Conference on Learning Representations (ICLR)*, 2022. arXiv:2106.09685.

[16] Christopher F. Brown, Michal R. Kazmierski, Valerie J. Pasquarella, William J. Rucklidge, Masha Samsikova, Chenhui Zhang, Evan Shelhamer, Estefania Lahera, Olivia Wiles, Simon Ilyushchenko, Noel Gorelick, Lihui Lydia Zhang, Sophia Alj, Emily Schechter, Sean Askay, Oliver Guinan, Rebecca Moore, Alexis Boukouvalas, and Pushmeet Kohli. AlphaEarth foundations: An embedding field model for accurate and efficient global mapping from sparse label data. arXiv:2507.22291, 2025.

[17] Sanjay Thasma, Yu-Hsuan Ho, and Ali Mostafavi. Beyond backscatter: AlphaEarth land-cover priors for rapid SAR flood segmentation across foundation backbones. arXiv:2606.29134, 2026.

[18] Brian A. Nosek, Charles R. Ebersole, Alexander C. DeHaven, and David T. Mellor. The preregistration revolution. *Proceedings of the National Academy of Sciences*, 115(11):2600–2606, 2018. doi: 10.1073/pnas.1708274114.

[19] Microsoft Open Source, Matt McFarland, Rob Emanuele, Dan Morris, and Tom Augspurger. microsoft/PlanetaryComputer: October 2022, 2022.

[20] Jean-François Pekel, Andrew Cottam, Noel Gorelick, and Alan S. Belward. High-resolution mapping of global surface water and its long-term changes. *Nature*, 540(7633):418–422, 2016. doi: 10.1038/nature20584.

[21] Daniele Zanaga, Ruben Van De Kerchove, Dirk Daems, Wanda De Keersmaecker, Carsten Brockmann, Grit Kirches, Jan Wevers, Oliver Cartus, Maurizio Santoro, Steffen Fritz, Myroslava Lesiv, Martin Herold, Nandin-Erdene Tsendbazar, Panpan Xu, Fabrizio Ramoino, and Olivier Arino. ESA WorldCover 10 m 2021 v200, 2022.

[22] Olaf Ronneberger, Philipp Fischer, and Thomas Brox. U-Net: Convolutional networks for biomedical image segmentation. In *Medical Image Computing and Computer-Assisted Intervention – MICCAI 2015*, volume 9351 of *Lecture Notes in Computer Science*, pages 234–241, 2015. doi: 10.1007/978-3-319-24574-4_28.

[23] Chuan Guo, Geoff Pleiss, Yu Sun, and Kilian Q. Weinberger. On calibration of modern neural networks. In *Proceedings of the 34th International Conference on Machine Learning*, volume 70 of *PMLR*, pages 1321–1330, 2017.

[24] John C. Platt. Probabilistic outputs for support vector machines and comparisons to regularized likelihood methods. In Alexander J. Smola, Peter Bartlett, Bernhard Schölkopf, and Dale Schuurmans, editors, *Advances in Large Margin Classifiers*, pages 61–74. MIT Press, 1999.

[25] Anastasios N. Angelopoulos, Stephen Bates, Adam Fisch, Lihua Lei, and Tal Schuster. Conformal risk control. In *International Conference on Learning Representations (ICLR)*, 2024. arXiv:2208.02814.

[26] Marco Saerens, Patrice Latinne, and Christine Decaestecker. Adjusting the outputs of a classifier to new a priori probabilities: A simple procedure. *Neural Computation*, 14(1):21–41, 2002. doi: 10.1162/089976602753284446.

[27] Sture Holm. A simple sequentially rejective multiple test procedure. *Scandinavian Journal of Statistics*, 6(2):65–70, 1979.